Adsorption 6, 337–347, 2000
© 2000 Kluwer Academic Publishers. Manufactured in The Netherlands.

Dynamic Adsorption of Vapours by Activated Carbons and by Polymer-Derived Adsorbents: 1. Adsorption at 0% R.H.

F. KARPOWICZ AND J. HEARN*
Department of Chemistry and Physics, Nottingham Trent University, Clifton Lane, Nottingham, NG11 8NS, England, UK

M.C. WILKINSON
Oak Apple House, Great Wishford, Salisbury, Wilts, SP2 0PA, England, UK

Abstract. The uptakes of volatile organic compounds from a nitrogen carrier gas at 0% R.H. onto packed beds of adsorbents have been measured by monitoring the effluent vapour concentration profile as a function of time. The profiles have been quantitatively fitted by a modified Bohart-Adams equation which was then integrated to yield the adsorbent capacities. Traditional activated carbons, carbonised macroreticular resins and a macroreticular polymer were used in the study. Performance in the dynamic tests has been related to the pore volume characteristics and surface areas determined from nitrogen adsorption isotherms. Whilst the extent of micropore filling basically increased as the sorbate boiling point increased and increased capacities reflected increased micropore volumes, these trends were interrupted by size exclusion and specific polar interaction effects.

Keywords: adsorbents, processes and applications

Introduction

Packed beds of adsorbents have long been used to remove volatile organic compounds from air streams in a variety of applications (Nonhebel, 1972) and remain the method of choice (Le Van, 1998). They may be used in end-of-pipe technology to prevent environmental pollution or to provide clean air for personnel either on an individual basis via a personal respirator, or collectively as in air conditioning. They may also be used to concentrate atmospheric pollutants prior to analysis (Karawacki et al., 1998) or for recovery by temperature swing adsorption (Boger et al., 1997) or pressure swing adsorption (Pezolt et al., 1997). Newer high surface area microporous adsorbents in the form of macroreticular resins and carbonised macroreticular resins are potential rivals (Rohm and Haas, 1992) for traditional coal-based or nutshell-based carbons in air filtration applications.

There is interest in small scalelaboratory experiments which can mimic the behaviour of full scale air filters (Smith, 1983) and also interest in characterisation procedures which may be able to predict dynamic performance (Abraham and Walsh, 1992) without the need to carry out such tests and so perhaps avoid the handling of toxic vapours.

In the studies reported here adsorbates were chosen to cover a wide range of volatilities. The adsorbents had moderate to high BET surface areas predictive of a good performance but were fundamentally different in nature. Traditional coal and nut-shell based carbons tend to lack the transport pores which may be retained when functionalised macroreticular resins are carbonised. Uncarbonised macroreticular resins may have high surface areas suggesting a micropore contribution to their general mesoporosity. Conventional carbons contain the highest level of polar functional groups whilst the carbonised resins would usually be synthesised to retain far lower levels and the polymeric material would be expected to display little surface polarity at all. These studies aim to try to elucidate any fundamental differences in the dynamic adsorption

characteristics of these different types of candidate materials for air filtration applications.

This paper reports dynamic adsorption experiments which have been carried out at 25°C and 0% R.H. in relation to adsorbent characterisation by nitrogen adsorption at 77 K and the associated surface areas and pore size distributions. The effects of a humid carrier gas have also been studied and will be reported later.

Experimental

Materials

Details of the adsorbents and adsorbates used are given in Tables 1 and 2 respectively. The adsorbents include traditional activated carbons—from a coal base —BPL,—from a nutshell base—SCII, an impregnated coal based carbon—Whetlerite, pyrolysed macroreticular resins—XEN series, and a polymeric macroreticular resin—XAD 4. The adsorbates were chosen to cover a wide range of boiling points and to be suitable for monitoring by an electron capture detector.

Test Procedure

Different bed depths (5–50 mm) of adsorbents were packed into 2 cm diameter volume activity, VA, tubes capped with wire mesh end pieces. The tubes were filled uniformly using a snowstorm filler device which caused particles, having been fed into a funnel, to impact with crosswires near its base and then to collide with one another and with the walls of the filler tube which was 24 cm in length. When the VA tube overflowed it was swept with a flat blade held flush to a reference plate. The tube was then capped, weighed and placed in a vacuum oven. Samples were left for a minimum of 3 hours at 120°C, with the exception of XAD 4 which was held at 70°C i.e. 20°C below its glass transition temperature, and were then allowed to cool overnight in the vacuum oven.

Samples in VA tubes were then introduced, one at a time, into the test apparatus illustrated in Fig. 1 at the position marked "Sample." The VA tube was mounted in a constant temperature water bath at 25°C ± 0.1°C, whilst the whole apparatus was housed in a temperature controlled cabinet. The carrier gas flow rate

Table 1. Details of adsorbents.

Adsorbent	Origin	Diameter/mm	Supplier
XAD 4	Cross-linked styrene/divinylbenzene	0.55 (34)[a]	Rohm & Haas
SGM1701-1 (SARO)	Carbonised polymer	0.64 (11)	Rohm & Haas
XEN 563	Carbonised polymer	0.64 (11)	Rohm & Haas
XEN 564	Carbonised polymer	0.51 (19)	Rohm & Haas
XEN 572	Carbonised polymer	0.56 (16)	Rohm & Haas
SCII	Coconut shell	12 × 30 mesh[b]	Chemviron
BPL	Coal based, steam activated	12 × 30 mesh	Chemviron
Whetlerite	Whetlerized version of material similar to BPL	12 × 30 mesh	Chemviron

[a]Values in parentheses are standard deviations as percentages.
[b]12 × 30 mesh ≡ 1.7 × 0.60 mm.

Table 2. Details of adsorbates.

Vapour	Relative pressure[a]	Boiling point/°C	Supplier
Sulphur hexafluoride	6.1×10^{-6}	−61 (sublimes)	Cambrian Gases
Freon 12 (CCl_2F_2)	5.8×10^{-5}	−29.8	Cambrian Gases
R114 ($C_2Cl_2F_4$)	1.1×10^{-4}	+3.8	Cambrian Gases
Methyl iodide	6.0×10^{-4}	+42.4	Lancaster Synthesis
Carbon tetrachloride	2.1×10^{-3}	+76.5	BDH
Iodobutane	1.3×10^{-2}	+130.5	Aldrich

[a]Relative pressure for vapour at 2 mg/dm^3.

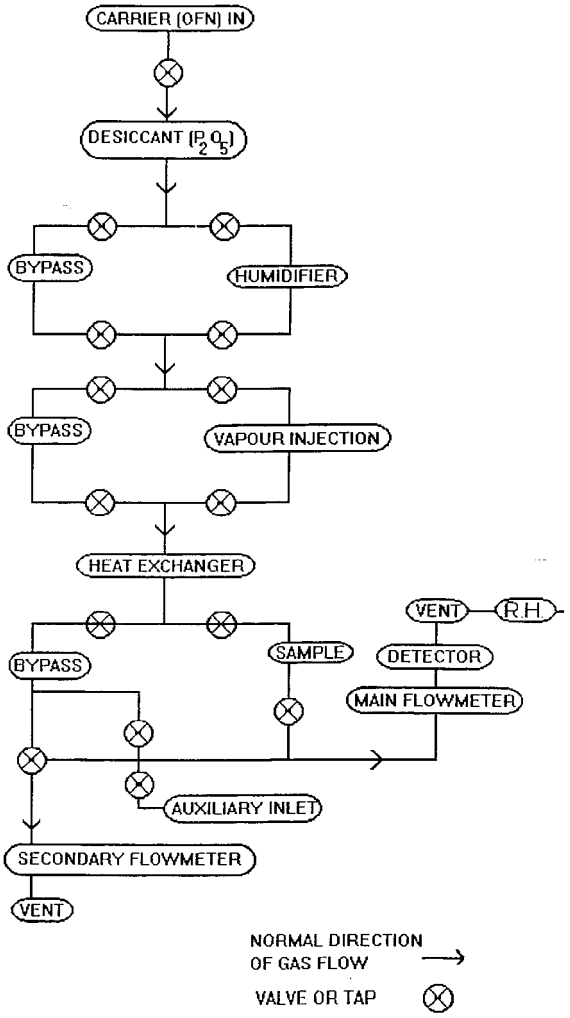

Figure 1. A schematic diagram of the dynamic adsorption apparatus.

(1 dm^3 per minute) and bed cross sectional area were chosen to mimic on a smaller scale those experienced in a typical 10 cm diameter respirator cannister at the breathing rate of a human at rest. The carrier stream of "white spot" nitrogen (also called "oxygen free nitrogen" containing <2 ppm oxygen as supplied by the British Oxygen Company, BOC) was passed over P_2O_5 to achieve a relative humidity of 0% and the vapour under test was introduced to maintain a concentration of 2 mg per dm^3. Adsorbates which were vapours at 25°C were injected directly using a gas tight syringe and syringe-drive, whilst the liquids, carbon tetrachloride and iodobutane, were injected into a port held at 100°C. The effluent vapour concentrations were monitored using a Leakmeter 125, (Analytical Instruments, Cambridge), electron capture detector. For a range of bed depths, effluent concentrations were monitored until they matched the influent concentration. No corrections were made for the dead space in the VA tube, but blank tests with SF_6 suggested that it contributed no more than 0.4 mg to the apparent uptake.

Adsorbent Characteristics

Nitrogen adsorption/desorption data at 77 K were obtained using a variety of experimental techniques and apparatus including a CI microbalance Mk 2, a Carlo Erba Sorptomatic and an Omnisorb 706 (Coulter Electronics) in order to obtain BET surface areas and pore size distibutions. Pore sizes in the macropore to meso pore ranges were also determined by mercury porosimetry (Carlo Erba 2000).

Results and Discussion

The BET surface areas, micropore volumes and combined macro plus mesopore volumes derived from nitrogen and mercury porosimetry data are shown in Table 3. Trends in the surface areas are mirrored in the magnitude of the the micropore volumes. Some adsorbents i.e. the traditional activated carbons plus XEN 572 and SGM were more effective than others i.e. the impregnated conventional carbon, the carbonised resins XEN 563 and XEN 564 and the XAD 4 polymeric resin. Greater volumes of transport meso and macro pores may be available in the polymer-derived materials where they had been synthesised with that characteristic in mind.

Table 3. Surface areas and pore volumes.

	Surface area/$m^2\ g^{-1}$	Micropore volume/$cm^3\ g^{-1}$	Meso + macropore volume/$cm^3\ g^{-1}$
XEN 572	1230	0.41	0.43
SCII	1225	0.43	0.03
BPL	1100	0.44	0.03
SGM	1097	0.43	0.09
XAD 4	806	0.29	0.89
Whet.	807	0.32	0.11
XEN 563	605	0.23	0.37
XEN 564	575	0.24	0.32

As the adsorbents used in this study are largely microporous, a means of measuring micropore size distributions would be useful and if these could be deduced from nitrogen isotherms it might then be possible to associate the adsorption of a given vapour with micropores of a particular size range. Once this had been done then measurement of the nitrogen isotherm of a novel adsorbent would allow the vapours against which it would prove effective to be deduced. The micropore size distributions in Figs. 2 and 3 are derived from the treatment of the low pressure section of Omnisorb nitrogen isotherms by a published method (Horvath and Kawazoe, 1983). This treatment assumes that, at a given relative pressure, all pores below a corresponding diameter are full of condensed sorbate and all larger pores are empty. The relationship between relative pressure and the parameter d is given by:

$$\ln\left(\frac{P}{P^0}\right) = \frac{62.38}{d - 0.64}\left[\frac{1.895 \times 10^{-3}}{(d - 0.32)^3} - \frac{2.7087 \times 10^{-7}}{(d - 0.32)^9} - 0.05014\right] \quad (1)$$

d is not equal to the pore diameter but rather is the distance between the nuclei of atoms on opposite sides of the pore. The effective pore size is obtained, for carbon micropores, by subtracting the diameter of a carbon atom, 0.34 nm, from d. For a series of values of d, the corresponding p/p^0 can be calculated from Eq. (1). The increasing uptakes at increasing p/p^0 values are assumed to be due to the filling of larger and larger pores with liquid adsorbate. The pore sizes calculated by Horvath and Kawazoe's method and an established method for determining mesopore size distributions (Dollimore and Heal, 1970) coincide at $p/p^0 = 0.05$ i.e. a diameter of 1.5 nm. Above this size Horvath and Kawazoe favoured Dollimore and Heal's method. Micropore size distributions for the XEN carbons and for SCII are shown in Fig. 2 and that for XAD 4 is shown in Fig. 3. All micropore size distributions showed a sharp peak at ca. 0.55 nm but in the case of XAD 4 this merged into a tail of larger pores up to the limit of the analysis at 1.5 nm. Surprisingly then, this method found pores smaller than would generally be associated with nutshell carbons i.e. between 1–2 nm diameter (Kinoshita, 1988) and found similar sized pores for all XEN carbons and a significant number of similarly sized pores for XAD 4. Others (Carrot et al., 1998) have also reported underestimates of micropore sizes using the Horvath and Kawazoe method.

Adsorbate Characteristics

Some adsorbate characteristics likely to influence their adsorption are shown in Table 4. Low uptakes are likely if adsorption is carried out close to the critical temperature (T_c) and a general increase in uptake with sorbate boiling point (T_b) might be expected. As the ability of activated carbons to adsorb a particular molecule can sometimes be changed drastically by slight heat treatment (Koresh and Soffer, 1980) this suggests that the dimensions of individual sorbates, as shown in the table, relative to the pore sizes of the adsorbents, may be important. Highly polar adsorbates, i.e. those with dipole moments comparable to or exceeding that of water, might be expected to be adsorbed strongly by polar sites on the more hydrophilic adsorbents (identified in Table 5 by their larger water uptakes under humid conditions), particularly at 0% R.H., when there is no competition for these sites from adsorbed water.

The critical temperature of SF_6 is over 20°C above the test temperature and it has no dipole moment. The attractive forces for this small molecule will be particularly low. Freon 12 has a higher T_c and dispersion forces are likely to be greater than for SF_6 and although it has a dipole moment it is small. The dipole moment for R114 is slightly higher than that for freon 12 but any increase in uptake is likely to be due to its increased dispersion forces. Its minimum cross sectional area is similar to that of freon 12. Methyl iodide has a significant dipole moment which is likely to lead to increased adsorption on to polar sites and its minimum cross section is small which may allow entrance to narrow pores. For carbon tetrachloride it has a critical temperature and a boiling point some 30°C above those for methyl iodide and it has no dipole moment; thus any increase in capacity would be due, almost entirely, to dispersion forces. Iodobutane has a large cross sectional area which may make transport through narrow pores slower and it has a higher dipole moment than water so that it may be strongly adsorbed by polar sites as well as by micropores.

Adsorption Profiles

An equation originally shown to give profiles of the correct qualitative shape (Bohart and Adams, 1920),

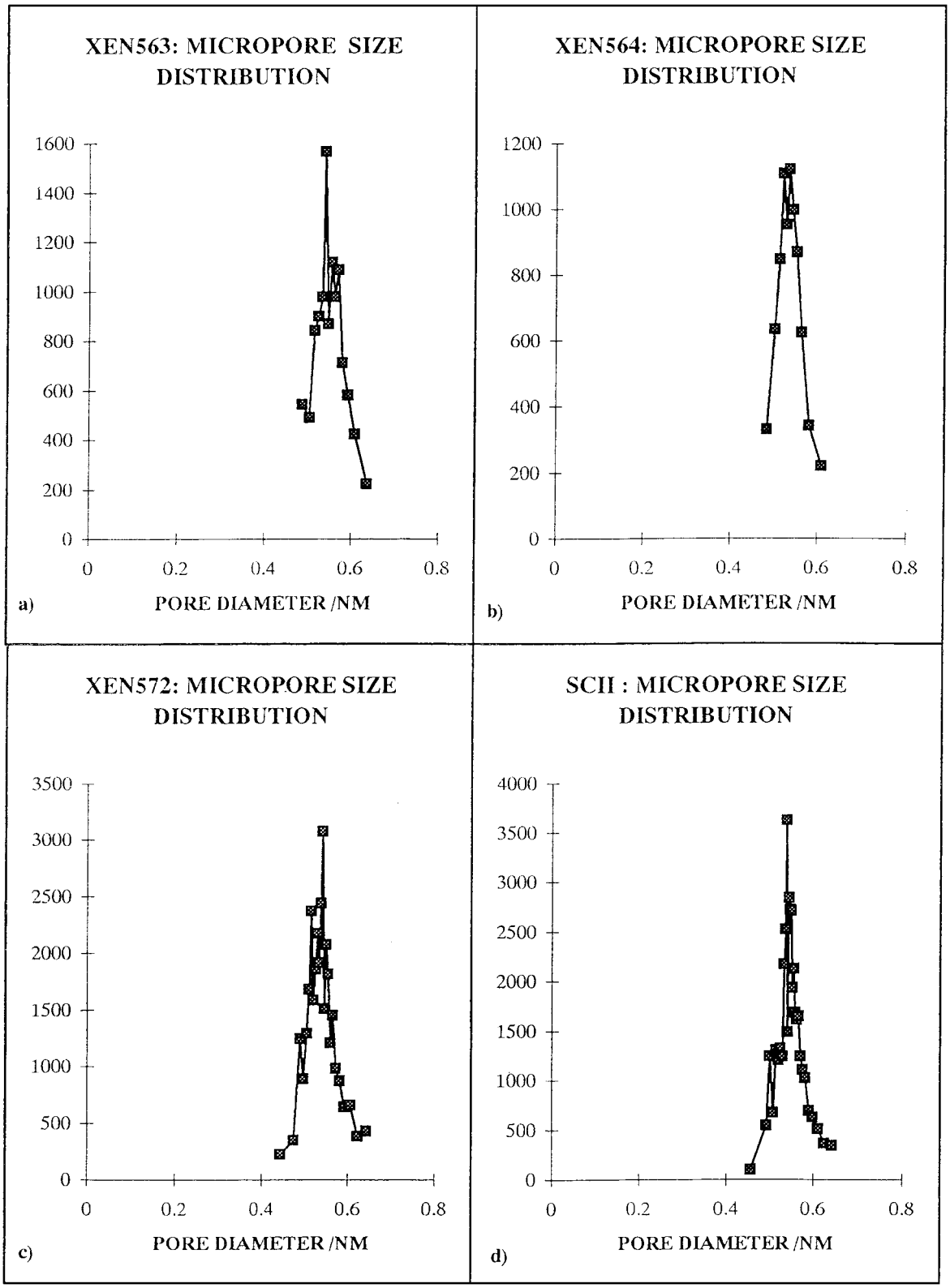

Figure 2. Differential micropore size distributions. (Abscissae: CM^3 Gas/G/Pore diameter/NM.)

Table 4. Properties of the test vapours.

	T_b/°C	T_c/°C	Dipole moment/debye	Radius (liquid)/Å	Min. cross-sectional area/Å^2	Max. cross-sectional area/Å^2
SF_6	−61	45.6	0	3.13	5.8	16.3
Freon12	−29.8	112	0.6	3.32	7.2	34.2
R114	3.8	145.7	0.8	3.60	7.2	42.5
CH_3I	44	254.8	1.65	2.91	2.8	29.7
CCl_4	77	283.1	0	3.37	10.3	47.3
C_4H_9I	130	250.7	2.12	3.57	35	154
H_2O	100	374.1	1.85	1.92	0.9	4.3
N_2	−195	−146.8	0	2.40	3.3	10.6

Table 5. Water uptakes (% g/g) at 80% R.H. (25°C).

Whet.	BPL	SCII	XEN 572	XEN 564	XEN 563	SGM	XAD 4
32	35	37	27	17	10	5.6	<1

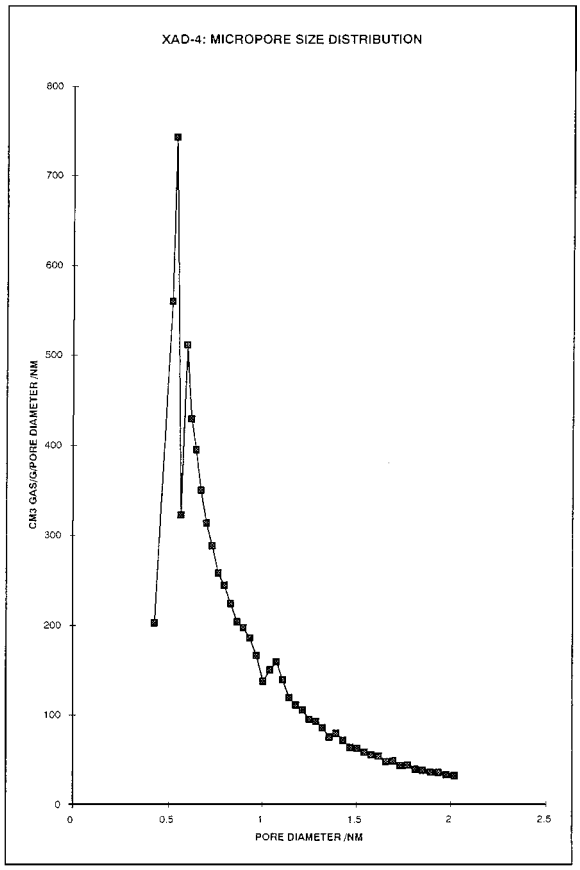

Figure 3. Differential micropore size distribution; XAD-4.

has been modified with respect to the velocity term used (Karpowicz et al., 1995), and shown to give excellent quantitative fits to sorbate effluent profiles:

$$\frac{C}{C_0} = \frac{e^{kC_0t}}{e^{kC_0t} + e^{\frac{kw}{F}} - 1} \tag{2}$$

Figure 4 shows a typical example of the fit given by the modified Bohart-Adams equation. Further modification of the equation to:

$$C = b + (C_0 - b)\frac{e^{kc_0t}}{e^{kc_0t} - 1 + e^{\frac{kW}{F} \times \frac{C_0}{C_0 - b}}} \tag{3}$$

where b is the concentration of vapour by-passing the sample e.g. in the void volume between the regular spheres of the XEN materials, then enables a good fit to be obtained here also as shown in Fig. 5. By-passing of this type i.e. by a proportion of the carrier gas stream, did not occur with the irregularly shaped carbon particles or with the more polydisperse spheres of XAD 4. The by-passing in the XEN carbons is believed to be due to the smooth nature of the uniform spheres which allow turbulence to decay more readily. The effect was not due to any lack of reproducibility in the overall packing density of these materials.

Only two parameters are required, in the absence of bypassing, to summarize an adsorption profile of the Bohart-Adams type i.e. the bed capacity and the rate constant k. Figure 6 shows the effect upon profile shape of varying k for a hypothetical adsorbent with a capacity of 500 mg challenged at 2 mg dm^{-3} min^{-1}. For a given capacity the higher the value of k the higher is the proportion of the capacity ultimately used at a given level of penetration and in the limit the profile becomes a step function. Being a kinetic factor, k may

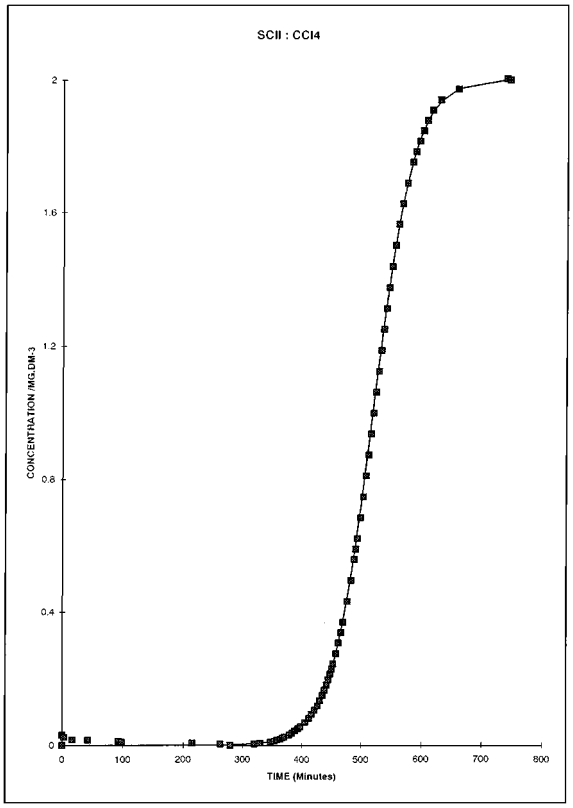

Figure 4. A Bohart/Adams profile (line) fitted to experimental points.

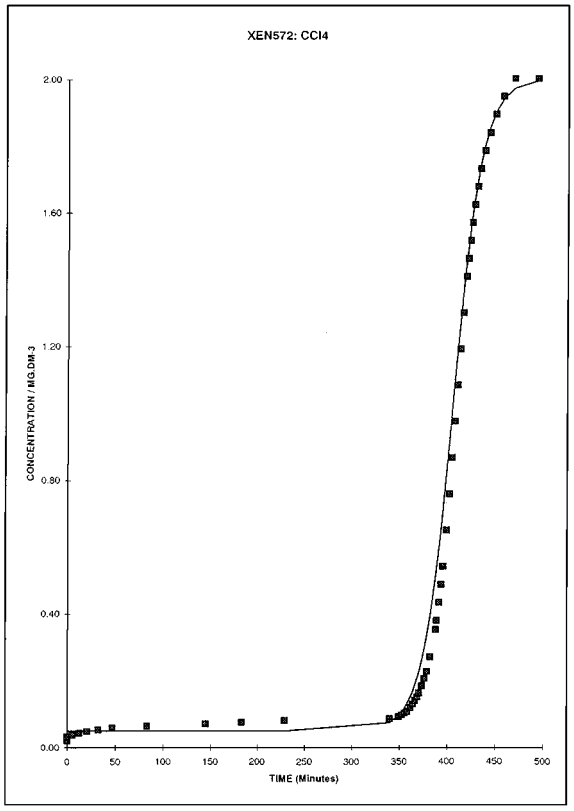

Figure 5. A Bohart/Adams profile fitted to experimental points with 'bypass'.

be limited by the readiness of access to the adsorbing sites. As shown in Table 6, although k decreased with increasing bed depth, presumably as a consequence of longer contact times in longer beds enabling a wider range of pores to be accessed, the differences in k values between carbons were small. Slightly higher values were found for XEN 564 and the highest values of all were found for XAD 4, the adsorbent which proved to have the lowest capacity. The high k values for XAD 4 may be due to the ready accessibility of its pores due to its high mesopore, transport pore, volume. The relatively high value of k for SF_6 adsorption in general, suggests ready accessability to a small proportion of the most retentive micropores or possibly adsorption on to surface sites only.

Capacities

The bed capacity, W, can be obtained by integrating the Bohart-Adams equation with respect to time (Karpowicz et al., 1995). The capacities for all the sorbate/sorbent combinations measured are shown in Table 7 and the percentage of the adsorbent's micropore volume occupied by sorbate, if liquified, are shown in parentheses. The uptakes of vapour are plotted separately for high and low capacity adsorbents as a function of sorbate boiling point in Fig. 7. The nitrogen adsorption isotherms used for characterising the adsorbents (based either on BET surface areas or micropore volumes) would predict broadly similar adsorption for SCII, BPL, Whetlerite, XEN 572 and SGM with XAD 4 showing slightly lower adsorption and XEN 564 and XEN 563 showing definitely lower adsorption. At the low p/p^0 challenge concentrations used it would be expected that the enhanced adsorption potential in micropores would principally be involved, and thus micropore volumes rather than BET surface areas would give the more useful correlation with sorbate uptake, particularly if the BET area included a large contribution from mesopore walls. Furthermore, the availability of the capacity at low concentrations

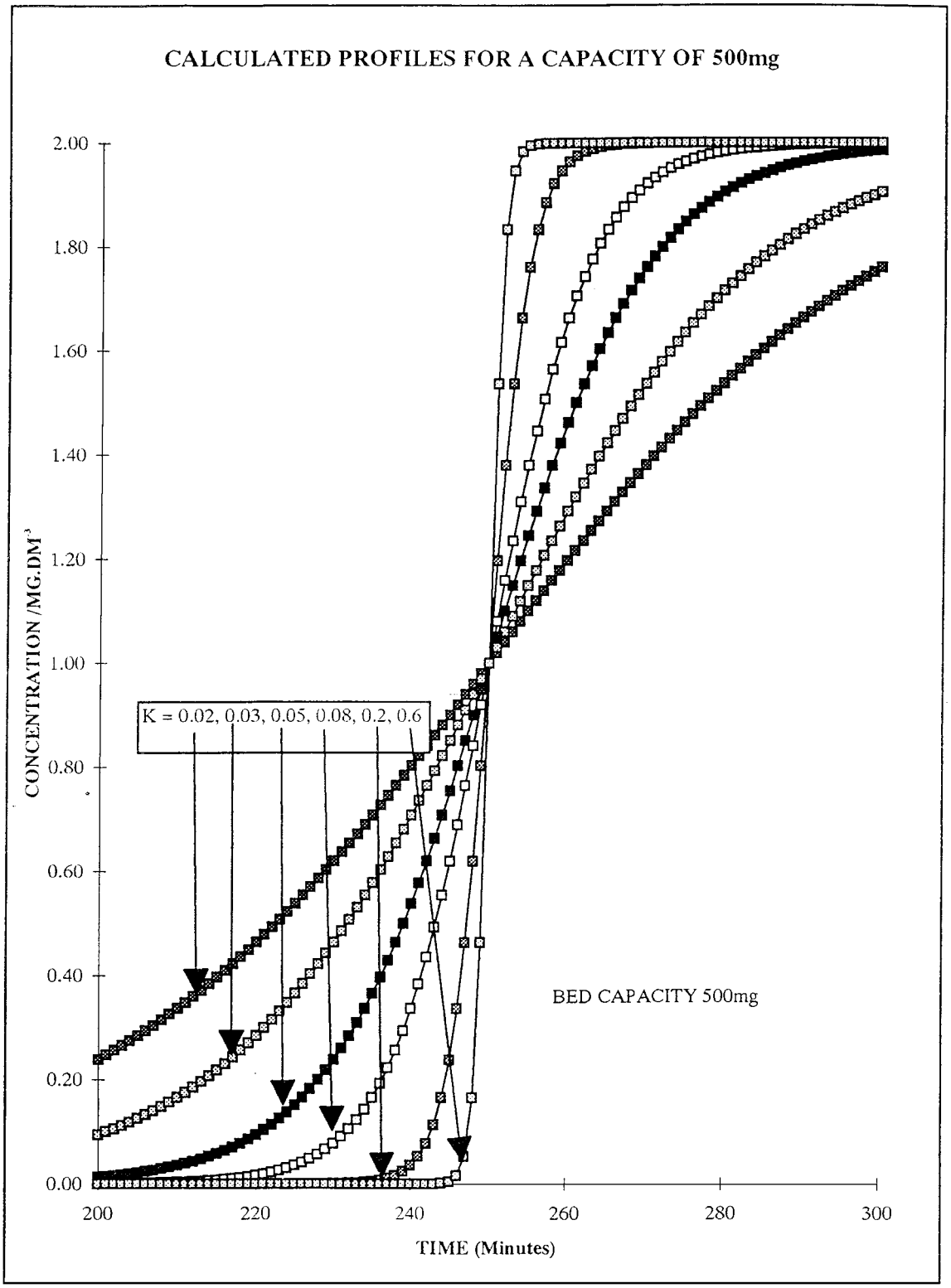

Figure 6. The effect of variations in 'K' on idealized Bohart/Adams adsorption profiles.

Table 6. A summary of the variation in *k* values with sorbent bed depth[a].

	SF_6	Freon12	CH_3I	CCl_4	C_4H_9I
BPL	370–107 (2–5)	70–20 (0.5–3)	35–12 (0.5–3)	33–13 (0.5–5)	5.5 (1)
Whet.	400–190 (2–5)	82–44 (0.5–2)	34–10 (0.5–2)	15.5–7.5 (0.5–3)	
SCII	350–120 (1–5)	35–20 (0.5–2)	44–11 (0.5–2)	24–7 (0.5–2)	8.5 (1)
XEN 572	350–200 (1–5)	45–22 (0.5–1.7)	35–4 (0.5–3)	80–11 (0.5–1.5)	7 (1)
XEN 564	1100–610 (1.5–5)	50–26 (1–4)	12–6 (0.5–2)	150–30 (0.5–2)	18 (1)
XEN 563	450–200 (1.5–4)	25–13 (1.5–2.5)	15–4 (0.5–5)	53–9 (0.5–4.5)	23 (1)
XAD 4		700–680 (4–5)	170–100 (3–5)	130–65 (0.5–2)	27 (1)

[a] $100k/dm^3\ g^{-1}\ min^{-1}$ (Depth/cm); bed depth ranges, in cm, are given in parentheses.

Table 7. Dynamic uptakes (in mg g^{-1}).

	SCII	XEN 572	BPL	SGM	Whet.	XAD 4	XEN 563	XEN 564
SF_6	4.5 (0.6)[a]	4.3 (0.5)	3 (0.4)		2.2 (0.4)		1.8 (0.4)	0.8 (0.2)
Freon12	82 (14.5)	70 (11.9)	55 (8.9)		38 (9.1)	0.95 (0.3)	55 (18.3)	28 (8.9)
R114	200 (31.8)	250 (38.2)	135 (19.6)		110 (23.5)	4 (1.1)	95 (28.3)	25 (7.1)
CH_3I	190 (19.4)	190 (18.6)	130 (12.1)	140 (14.3)	128 (17.6)	9 (1.7)	180 (34.5)	165 (30.3)
CCl_4	370 (54.1)	320 (44.8)	290 (38.6)	334 (48.9)	275 (54.1)	32 (8.4)	130 (35.5)	32 (8.4)
C_4H_9I	671 (96.7)	552 (76.4)	560 (74.4)	560 (80.9)	307 (59.6)	144 (37.3)	260 (70.2)	280 (59.6)

[a] Percentages of the micropore volumes occupied are given in parentheses.

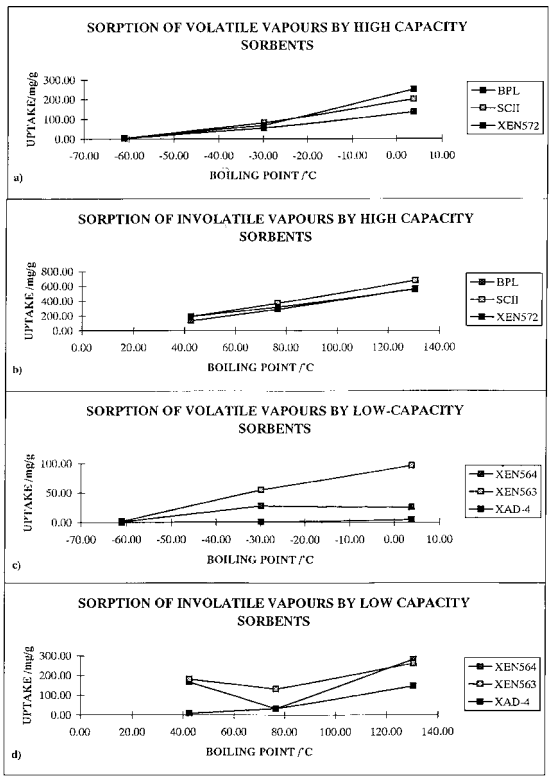

Figure 7. Uptakes of vapours by the main sorbents.

Table 8. The increase in the CCl_4 capacity of XEN 563 with bed depth.

Bed depth/cm	Sample weight/g	Packing density/g cc^{-1}	Uptake/ mg g^{-1}
0.5	0.8972	0.571	70.0
1.0	1.6497	0.525	85.3
3.0	5.3365	0.566	125.0
4.0	8.1082	0.574	130.0

becomes even more important as the boiling point of the sorbate decreases when mesoporosity may only influence transport rates. There is the expected general trend of increasing uptake with increase in sorbate boiling point and a commensurate increase in the proportion of the micropore volume occupied. The capacities of XEN 563 and XEN 564 for CCl_4 appear anomalously low. The XEN 563 capacity (g/g) for CCl_4 increased with bed depth, Table 8, which was not the case for other adsorbents and it is the capacity at the longest bed depth which is quoted in Table 7. As XEN 563 and XEN 564 have comparable surface areas and comparable butyl iodide capacities, the low uptake of CCl_4 by XEN 564 suggests that it is largely excluded from its micropore volume whilst the increase in uptake of CCl_4

with bed depth by XEN 563 suggests that its micropore volume is available albeit with difficulty. It has previously been suggested (Dacey and Thomas, 1954) that there are transport problems for the bulky CCl_4 molecule in microporous carbons. CH_3I uptakes on the more polar sorbents are low and it seems that adsorption on to the polar sites may hinder access, possibly as a consequence of the bulky iodine atom, to some of the micropore volume. It is apparent, even at the low relative pressures used here, that the adsorbents pore characteristics do have a significant influence upon uptakes. This is in marked contrast with the findings from studies on the Henry's Law region of adsorption and their use to predict performance, when the nature of the adsorbent had little effect and especially there was no correlation with the BET surface areas (Maurer and Mersmann, 1998).

Desorption Profiles

SF_6 desorption from all the adsorbents, with the exception of XEN 564, and freon 12 desorption from XAD 4, were the only profiles to show mirror images of their Bohart-Adams adsorption. Less volatile vapours produced curves which could be fitted by expressions of the type:

$$\log(C) = A - B[\log(t)]^N \qquad (4)$$

where A and B are constants and N is an empirical exponent.

Desorption profiles are shown in Fig. 8 for the most strongly retained vapour, iodobutane, from XEN 564, BPL and XAD 4 indicating 20%, 55% and 100% removal respectively. For vapours more volatile than CCl_4 100% desorption into a clean nitrogen stream at ambient temperature could be achieved within 5 hours from the conventional carbon SCII and from XEN 572. With carbon tetrachloride and iodobutane desorption was not complete after 24 hours. Adsorbents XEN 564 and XEN 563 appeared more retentive. XEN 564 still retained ca. 15% SF_6 and ca. 30% R114, CH_3I and CCl_4 when desorption had dropped below a detectable rate. As freon 12 desorbed completely from all sorbents, the retention, by XEN 564, of some of the lower boiling SF_6 (or its release at too slow a rate for detection), suggests that some of the micropores in XEN 564 might be small enough to exclude freon 12, while admitting SF_6; both types of tetrahedral face in freon 12 have larger cross sectional areas than does an octahedral face of SF_6. In the case of XEN 563 transport problems suggested by

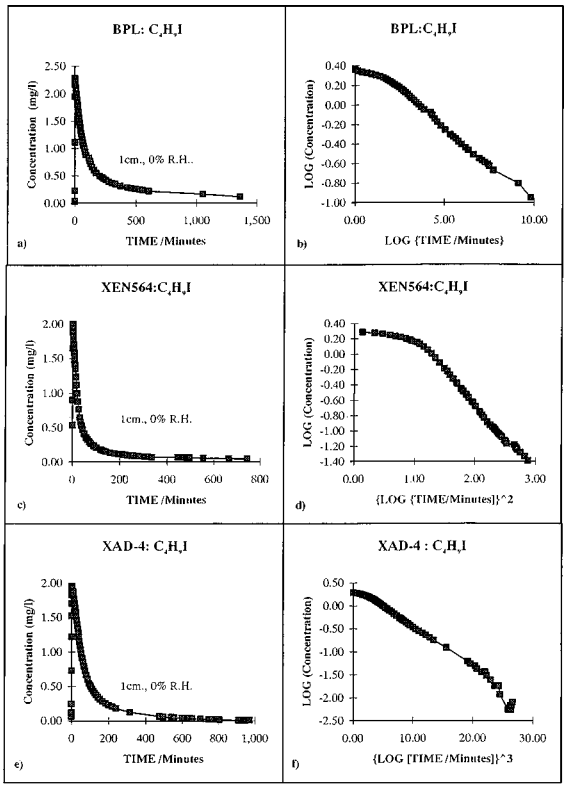

Figure 8. Iodobutane desorption profiles.

the increase in capacity per gram with bed depth for CCl_4, may also apply to desorption and make this adsorbent appear more retentive than it actually is. The Horvath and Kawazoe treatment which suggested that micropores in all carbons occurred at 0.55 nm failed to discriminate between systems consisting of (i) pores large enough for CCl_4 to enter (SCII and XEN 572), (ii) a mixture of pores not all of which are available for CCl_4 sorption (XEN 563) and (iii) pores from which CCl_4 is largely excluded (XEN 564).

Conclusions

The usefulness of a modified Bohart-Adams equation to describe adsorption profiles of organic vapours on to packed beds of adsorbents has been demonstrated. For a fixed carrier flow rate and inlet vapour concentration, the theoretical profile depends only on the total capacity of the adsorbent at full penetration and a kinetic factor, k, that governs the steepness of the rise of the adsorption profile, which is symmetrical about the 50% breakthrough time. The higher the value of k, the

steeper is the rise in the profile and the greater is the proportion of the total capacity used prior to any given level of breakthrough.

Comparison of the nitrogen adsorption isotherms especially in the region of micropore filling, allows the possible usefulness of adsorbents to be assessed but pore entry problems for organic vapours can then complicate the picture.

The increase in the capacities of the carbons with increasing sorbate boiling point was interrupted from R114 to CH_3I and for the most retentive carbons (XEN 564 and XEN 563), reversed, probably by size exclusion, when CCl_4 succeeded CH_3I. Although the capacity of XAD 4 for the sorbates increased with increasing sorbate boiling point, XAD 4 had the lowest uptake of any of the sorbents for any of the vapours. XAD 4 was also the least retentive adsorbent shown e.g. by the ability of Bohart-Adams equations to describe the desorption of freon 12.

The XEN carbons were far more susceptible than the conventional ones to fast penetration, before their capacity was utilised, due to their nature as smooth uniform spheres. If allowance was made for by-pass in the equations describing the adsorption profiles then the values of the kinetic term, *k*, were similar for conventional carbons and the carbonaceous resins XEN 563 and XEN 572 but slightly higher for XEN 564. Of the XEN carbons, XEN 572 has capacities similar to those of SCII and slightly higher than those of BPL, Whetlerite and SGM. Lower capacities were found for XEN 563 and XEN 564. The capacity of XEN 564 for CCl_4 is unusually low and, taken with its ability to retain a higher proportion of SF_6, CH_3I, CCl_4 and C_4H_9 (when the desorption rate has dropped below the detection limit), than any other sorbent, suggests that the micropores in XEN 564 are small whilst XEN 563 too may contain some small pores. The provision of a larger population of transport pores appears to offer no advantage, in terms of the percentage of micropore capacity utilized by these materials, during dynamic adsorption at 0% R.H.

Nomenclature

C_0 is the vapour concentration (mg dm^{-3}) in the supply
C is the effluent vapour concentration (mg dm^{-3})
k is a rate constant (mg^{-1} dm^3 min^{-1})
t time (min)
F the volumetric flow rate (cm^3 min^{-1})
W is the bed capacity (g) i.e. the total weight of adsorbate taken up under dynamic conditions
b is the vapour concentration (mg dm^{-3}) in the supply which by-passes the adsorbent

References

Abraham, M.H. and D.P. Walsh, "Hydrogen Bonding-23. Application of the New Solvation Equation to Log V(G) Values for Solutes on Carbonaceous Adsorbents," *Journal of Chromatography*, **627**(1, 2), 294–299 (1992).

Boger, T., A. Salden, and G. Eigenberger, "A Combined Vacuum and Temperature Swing Adsorption Process for the Recovery of Amines from Foundry Air," *Chem. Eng. Process*., **36**, 231–234 (1997).

Bohart, G.S. and E.Q. Adams, "Some Aspects of the Behaviour of Charcoal with Respect to Chlorine," *J. Am. Chem. Soc*., **42**, 523 (1920).

Carrot, P.J.M., M.M.L. Riberio Carrot, and T.J. Mays, "Comparison of Methods for Estimating Micropore Sizes in Active Carbons from Adsorption Isotherms," in *Fundam. of Adsorption*, F. Meunier (Ed.), pp. 766–682, Elsevier, Paris, 1998.

Dacey, J.R. and D.G. Thomas, "Adsorption on Saran Charcoal, a New Type of Molecular Sieve," *Faraday Transactions*, **50**(7), 740–748 (1954).

Dollimore, D. and G.R. Heal, "Pore Size Distribution in Typical Adsorbent Systems," *J. Colloid & Interf. Science*, **33**(4), 508–519 (1970).

Horvath, G. and K. Kawazoe, "Method for the Calculation of Effective Pore Size Distributions in Molecular Sieve Carbons," *J. Chem. Eng. Japan*, **16**(6), 470–475 (1983).

Karawacki, C.J., L.C. Buettner, J.H. Buchanan, J.J. Mahle, and D.E. Tevault, "Low Concentration Adsorption Studies for Low Volatility Vapours," in *Fundam. of Adsorption*, F. Meunier (Ed.), pp. 315–320, Elsevier, Paris, 1998.

Karpowicz, F., J. Hearn, and M.C. Wilkinson, "The Quantitative Use of the Bohart-Adams Equation to Describe Effluent Vapour Profiles from Filter Beds," *Carbon* **33**(11), 1573–1583 (1995).

Koresh, J. and A. Soffer, "Study of Molecular Sieve Carbons Part I—Pore Structure, Gradual Pore Opening and Mechanism of Molecular Sieving," *J. Chem. Soc. Faraday I*, **76**, 2457–2471 (1980).

Kinoshita, K., *Carbon: Electrochemical and Physicochemical Properties*, pp. 10–15, Wiley & Sons, New York, 1988.

Le Van, M.D., "Adsorption Processes and Modeling: Present and Future," in *Fundam. Adsorption*, F. Meunier (Ed.), pp. 19–29, Elsevier, Paris, 1998.

Maurer, S. and A. Messmann, "Prediction of Henry's Law Constants for Gases and Vapours on Industrial Adsorbents," in *Fundam. Adsorption*, F. Meunier (Ed.), pp. 297–302, Elsevier, Paris, 1998.

Nonhebel, G., *Gas Purification Processes for Air Pollution Control*, Newnes-Butterworths, London, 1972.

Pezolt, D.J., S.J. Collick, H.A. Johnson, and L.A. Robbins, "Pressure Swing Adsorption for VOC Recovery at Gasoline Loading Terminals," *Environmental Progress*, **16**, 16–19 (1997).

Rohm and Haas Company, "Ambersorb Carbonaceous Adsorbents, Technical Notes," 1992.

Smith, M.E., "The Adsorption of Pulses of Vapours Through Charcoal Beds," M.Phil. Thesis, C.N.A.A., 1983.